Thermochimica Acta, 8 (1974) 409–421

A SIMPLE DIRECT-REACTION CALORIMETER AND SOME OBSERVATIONS ON THE HEATS OF FORMATION OF IIIA–VB SODIUM CHLORIDE STRUCTURES

K. S. CHUA* AND J. N. PRATT

Department of Physical Metallurgy & Science of Materials, University of Birmingham, P.O. Box 363, Birmingham B15 2TT (England)

(Received 27 August 1973)

ABSTRACT

The design and operation of a simple direct-reaction calorimeter, suitable for the study of highly exothermic reactions, is described. New experimental data for the heats of formation of ScSb, YSb, LaSb and LuSb are reported. Published lattice parameters of the IIIA–VB NaCl structures are used to calculate the effective homopolar and heteropolar energy gaps (E_h and C_{AB}) and fractional ionic character (f_i) of these phases and the stabilities of the phases are discussed in relation to these. An empirical relation is established between the observed heats of atomisation and Phillips' concept of ionicity of bonding and this is used to estimate values of the heats of formation of the phosphides and bismuthides of the IIIA metals and also that of LuN.

INTRODUCTION

The factors affecting the choice of fourfold or sixfold coordination in the crystal structures of A^NB^{8-N} phases have been examined by various authors[1,2]. Quantitative discussion of the relative stability is, however, inhibited by the lack of appropriate thermodynamic data for many of the systems concerned. Thus, for example, while the classic IIIB–VB adamantine semi-conductor compounds have been the subject of numerous thermodynamic investigations[3], comparatively little attention has been paid to the thermodynamics of formation of the large family of NaCl phases formed by the Group IIIA metals (including the Rare Earths) when combined with Group VB elements. Studies of these are of interest in relation to the fundamental problem of phase stability and also because they may include some of potential value as semi-conductor materials[4]. Thermodynamic data are available for a few of the nitrides[5] and a comprehensive study of the heats of formation of the arsenides has been reported by Faktor and Hanks[6]. Similar studies of the heavy rare-earth antimonides have been made by the present authors[7], using the direct-reaction calorimeter described here. The variation of behaviour across the rare earth

*Now at Department of Civil Engineering, University College, London, England.

series is complex and will be discussed in a separate publication; the present paper is concerned with the compounds of those Group IIIA metals which do not involve any incomplete sub-valency levels, i.e. Sc, Y, La and Lu. New experimental data are reported for the heats of formation of the antimonides of these and an empirical analysis of the probable variation of bond character is used to predict the corresponding quantities for the phosphides and bismuthides.

THE CALORIMETER

A calorimeter similar to some previous designs[8], but with a modified mode of operation, has been evolved. In its present form it is a single cell unit designed for the study of vigorous exothermic reactions. The instrument is shown diagramatically in Fig. 1. It is enclosed within a cylindrical vacuum chamber (A) provided with an enveloping water jacket. The chamber is evacuated, through the tube (B) at the centre of the base plate, by means of a 2.5 cm oil-diffusion pump and two-stage backing pump; the vacuum is monitored by means of Penning gauge. The vacuum

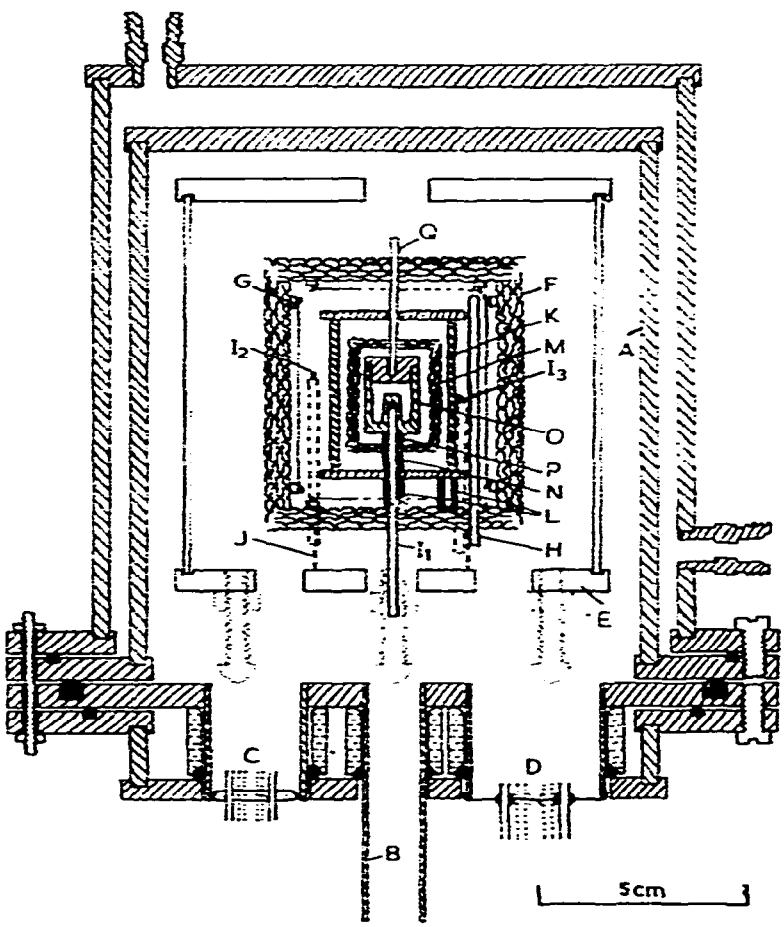

Fig. 1. Schematic diagram of the direct-reaction calorimeter.

chamber is mounted directly on top of the baffle valve and diffusion pump. Glass-metal seals (C and D) are fitted in the base plate of the vacuum chamber to provide lead-through for thermocouples and heater element connections. Within the vacuum enclosure stands a steel platform (E), with cylindrical body and cover; this supports the calorimeter proper and provides thermal shielding.

At the heart of the calorimeter is the cylindrical tantalum reaction cell (C). It is tightly closed with a screwed top which contains a central well to accommodate the calibration heater (Q); the heater consists of 5 mm long coil of fine tantalum wire and has a resistance of approximately 6 ohms. The base of the reaction cell is provided with a re-entrant thermocouple well so that the specimen thermocouple (I_1) is at the centre of the reaction region; the cell is totally enclosed by the inner radiation shields, formed from 0.05 mm thick tantalum sheets, dimpled to minimize contact. These are in turn enclosed in a heavier concentric heat shield (K) which consists of a circular tantalum base and top and cylindrical body (2.6 cm diameter, 4 cm high and 2 mm wall thickness). This body of higher thermal mass provides the isothermal enclosure of the calorimeter and the monitor thermocouple (I_3) is located in a hole drilled in the outer wall of the cylindrical body. The isothermal heat shield is entirely surrounded by the furnace enclosure (F), which comprises one (inner) tantalum and four (outer) molybdenum radiation shields, again constructed from dimpled 0.05 mm thick sheet. The heating element consists of exposed 0.2 mm diameter tantalum wire attached, by means of small alumina supports (G), to the inside of the innermost shields of the furnace enclosure and distributed over the side walls, base and top. The five main parts of the calorimeter proper, when assembled, are separated by thick-walled alumina tubes (L, N & P) and the thin-walled molybdenum cylinder (J) perforated further to reduce conduction.

The furnace temperature is controlled by means of a saturable-core reactor activated by a 6.5 ohm platinum resistance thermometer (H). Because of the low resistance of the furnace element (23 ohm) the input voltage to the saturable reactor is stepped down by means of an autotransformer to provide adequate sensitivity of control. The furnace temperature can be controlled within $\pm 0.5°$ and from 150–1650°C; the controller may be by-passed for rapid heating. In present operations, which are confined to temperature below 1000°C, the temperatures of the reaction cell, of the isothermal heat shield, and of the furnace are measured by means of three calibrated chromel–alumel thermocouples (I_1, I_2 and I_3) respectively; these are used in conjunction with a Tinsley vernier potentiometer or Rikadenki integrating recorder. The calibration heater is supplied from a stabilized d.c. supply and the power input measured using a standard resistance bridge circuit and the vernier potentiometer.

OPERATING PRINCIPLES

Although a single cell calorimeter, the mode of operation is essentially similar to that of differential thermal analysis. Programmed temperature control is not,

however, involved; the technique relies on the observation that exactly reproducible heating rate profiles can be obtained in the reaction cell simply by the choice of control temperature of the furnace and isothermal jacket. This behaviour is a consequence of the fact that the comparatively low thermal mass furnace and isothermal jacket achieve equilibrium control temperature (T_f) very rapidly, whereafter the reaction cell heats at a rate proportional to the difference between cell and furnace temperature; the cell eventually attaining a characteristic equilibrium temperature (T_{eq}) slightly below T_f. The technique is based on the observation of the cell temperature changes during runs with and without reaction, but under otherwise identical conditions.

Since heat transfer to and from the reaction cell may involve both conduction and radiation, the heating of the cell, when no reaction is taking place (reference run), may be described by the general equation

$$W\frac{dT}{dt} = K_1(T_f - T) + K_2(T_f^4 - T^4) - K_3(T - T_j) \tag{1}$$

where W is the heat capacity of the reaction cell plus contents, T, T_f and T_j are respectively the reaction cell, isothermal jacket and outer cooling jacket temperature, K_1 and K_2 the coefficients for conduction and radiation between reaction cell and furnace, K_3 the coefficient for heat loss by conduction down radiation shield supports, thermocouples and calibration heater leads and t is time.

When a reaction is taking place (reaction run), the above equation becomes

$$W\frac{d(T+\Delta T)}{dt} = -\frac{dQ}{dt} + K_1[T_f - (T+\Delta T)] + K_2[T_f^4 - (T+\Delta T)^4] - K_3[(T+\Delta T) - T_j] \tag{2}$$

where Q is the enthalpy of reaction of the sample and ΔT is the change in temperature of reaction cell and contents relative to the corresponding reference run temperature T.

Provided that $\Delta T \ll T$, so that terms involving powers of ΔT greater than one may be neglected, combination of eqns. (1) and (2) leads to the relation

$$W\frac{d\Delta T}{dt} = -\frac{dQ}{dt} - (K_1 + K_3 + 4K_2T^3)\Delta T. \tag{3}$$

Calibration experiments and the analysis of reference run heating characteristics demonstrate that, provided experimental conditions are suitably chosen, the expression $(K_1 + K_3 + 4K_2T^3)$ may reasonably be treated as constant over the period of the reaction, so that eqn. (3) may be written as

$$W\frac{d\Delta T}{dt} = -\frac{dQ}{dt} - K\Delta T \tag{4}$$

which by integration over the period of the complete reaction gives

$$-Q = W\Delta T + K\int_0^t \Delta T\,dt. \tag{5}$$

The value of K/W for an individual run can be evaluated from the post-reaction behaviour; in this period $dQ/dt = 0$ so that eqn. (4) becomes

$$W\frac{d\Delta T}{dt} = -K\Delta T \tag{6}$$

which by rearranging and integration yields

$$\ln \Delta T = -\frac{K}{W}t + \text{constant}. \tag{7}$$

The value of K/W is thus obtained from a plot of $\log \Delta T$ against t for the post-reaction period; the onset of linearity indicates the termination of reaction and provides an internal check on the validity of the approximations involved in the above treatment. Typical reaction and reference runs and the corresponding ΔT and log plots are shown in Fig. 2.

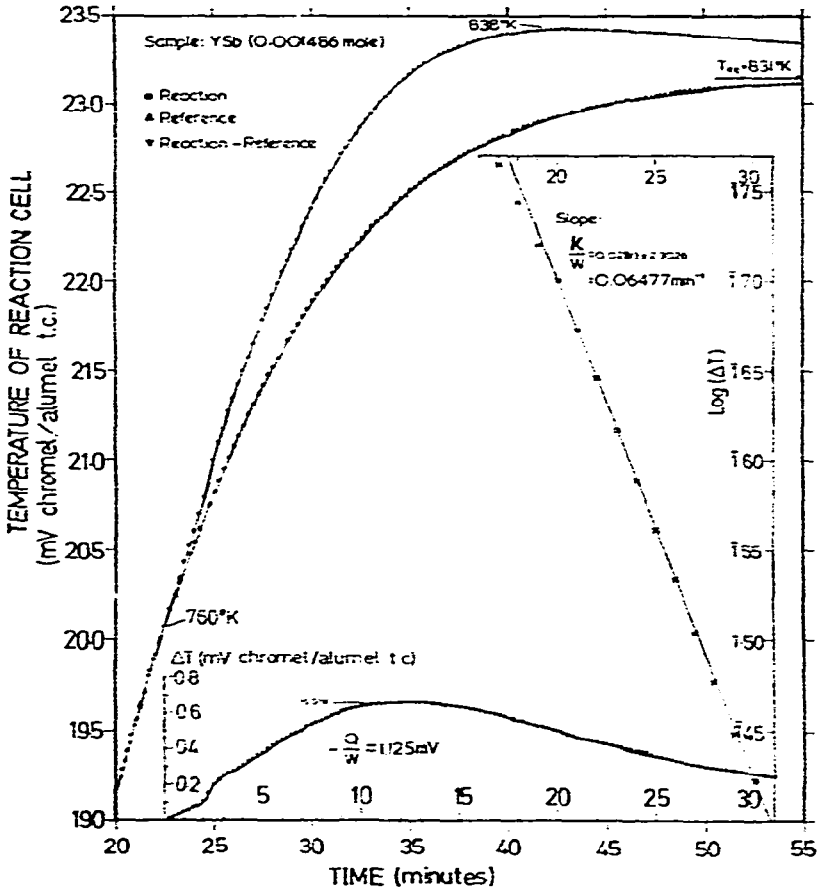

Fig. 2. Experimental runs: YSb sample.

The heat capacity (W) of the reaction cell and its contents is determined by the following calibration procedure. With the furnace controlled at a chosen temperature (T_f), the cell will settle to a unique equilibrium temperature (T_{eq}). Since in this state $dT/dt = 0$, one may write, from the general heat transfer equation in the absence of reaction (eqn. (1))

$$0 = K_1(T_f - T_{eq}) + K_2(T_f^4 - T_{eq}^4) - K_3(T_{eq} - T_j) \tag{8}$$

If a small heat effect, $(dQ/dt)_s$, is introduced into the reaction cell by means of the calibration heater, the cell temperature gradually rises to a new equilibrium temperature $T_{eq} + \Delta T_{eq}$, but eventually reverts to T_{eq} when the power is switched off. During the calibration heating the behaviour of the reaction cell may be described by the equation

$$W\frac{d\Delta T}{dt} = -\left(\frac{dQ}{dt}\right)_s + K_1[T_f - (T_{eq} + \Delta T)] + K_2[T_f^4 - (T_{eq} + \Delta T)^4]$$

$$- K_3[(T_{eq} + \Delta T) - T_j] \tag{9}$$

where $\Delta T = T - T_{eq}$. Combining eqns. (8) and (9) and again ignoring terms involving powers of ΔT higher than the first then yields

$$W\frac{d\Delta T}{dt} = -\left(\frac{dQ}{dt}\right)_s - K\Delta T \tag{10}$$

where here $K = (K_1 + K_3 + 4K_2T_{eq}^3)$. When the new equilibrium temperature is reached $\Delta T = \Delta T_{eq}$ and $d\Delta T/dt = 0$ so that the above equation becomes

$$-\left(\frac{dQ}{dt}\right)_s = K\Delta T_{eq} \tag{11}$$

while, for the post-calibration cooling when $(dQ/dt)_s = 0$, integrating eqn. (10) again yields

$$\ln \Delta T = -\frac{K}{W}t + \text{constant}. \tag{12}$$

From the observed temperature changes following a series of different power inputs to the calibration heater, plots of eqns. (11) and (12) permit the evaluation of K and K/W and hence of W.

EXPERIMENTAL PROCEDURE

Samples were prepared from antimony (99.99% purity) and scandium, yttrium and lutetium (>99.8% purity) supplied by Johnson–Matthey and Co. Ltd. Antimony was crushed to a fine powder and filings of the other elements prepared under carbon tetrachloride. The components were weighed separately and thoroughly mixed together with antimony very slightly in excess of the equiatomic ratio. The mixture

was then transferred to the reaction cell; amounts of sample corresponding to about 0.001–0.002 moles of compound were usually employed. The cell was immediately closed tightly, the apparatus set up as rapidly as possible and immediately evacuated to a vacuum better than 10^{-5} torr. Pumping was normally continued overnight to ensure adequate degassing before beginning heating.

With each compound a preliminary investigation was made to establish the temperature at which reaction between the components initiated. In subsequent runs the furnace was then controlled to produce an equilibrium maximum temperature approximately 50° above the initial reaction temperature; this has been found to produce optimum experimental conditions for the present technique. For a reaction run, after loading with a fresh mixture of the components and evacuating, the controller is set at the chosen temperature, the main heater switched on and the heating of the reaction cell is monitored until its temperature is approximately 150° below the control temperature. Detailed recording of its temperature is then commenced and continued through the reaction and post-reaction periods until the final maximum equilibrium temperature (T_{eq}) is reached. The calorimeter is then switched off and allowed to cool to the original ambient temperature, when the heating procedure is repeated under identical temperature control conditions; the heating of the cell then recorded in the absence of reaction constitutes the reference run. For calibration purposes the furnace temperature is set at temperatures below that used in the reference and reaction runs so that the reaction cell settles at points within the reaction range. Once stable, various inputs are supplied to the auxiliary heater and the calibration measurements performed. On completion of the experiments, samples are removed from the reaction cell and the nature of the reaction product checked by Debye–Scherrer analysis.

EXPERIMENTAL RESULTS

Calibration measurements were made at a series of temperatures within the range over which the reactions to form ScSb and YSb were observed to take place. The dependence of the temperature increment, ΔT_{eq}, on the power input to the calibration heater observed in these experiments is shown by Fig. 3; data obtained at different equilibrium temperatures (T_{eq}) between 787 and 820 K are included in this diagram. The linearity of this plot, or alternatively the constancy of K (calculated from the individual points) and of K/W (from the post-calibration cooling), demonstrate that the treatment of $(K_1+K_3+4K_2T^3)$ as a constant is justified. The value of K obtained by least square analysis of the data of Fig. 3 was found to be 0.675 J s^{-1} mV^{-1} or 0.161 cal s^{-1} mV^{-1}, with a standard deviation of 1%. Combining this with K/W values obtained from plots of eqn. (12) for post-calibration cooling established the heat capacity of the reaction cell and contents to be 73 cal mV^{-1} or 2.9 cal K^{-1}, again with an estimated uncertainty of $\pm 1\%$. The value of W is determined almost entirely by the mass of the tantalum reaction cell, which is large (30.445 g) compared with that of the samples, and so has been found to be virtually

invariant from run to run. Slight random variations of the heat transfer coefficient, K, have been found to result from minor differences in the calorimeter assembly between different investigations. To eliminate this possible source of error, without the need for detailed re-calibration each time, values of K/W and hence K are obtained from post-reaction behaviour in individual runs and these are employed in evaluating the heats of reaction (Q) using eqn. (5).

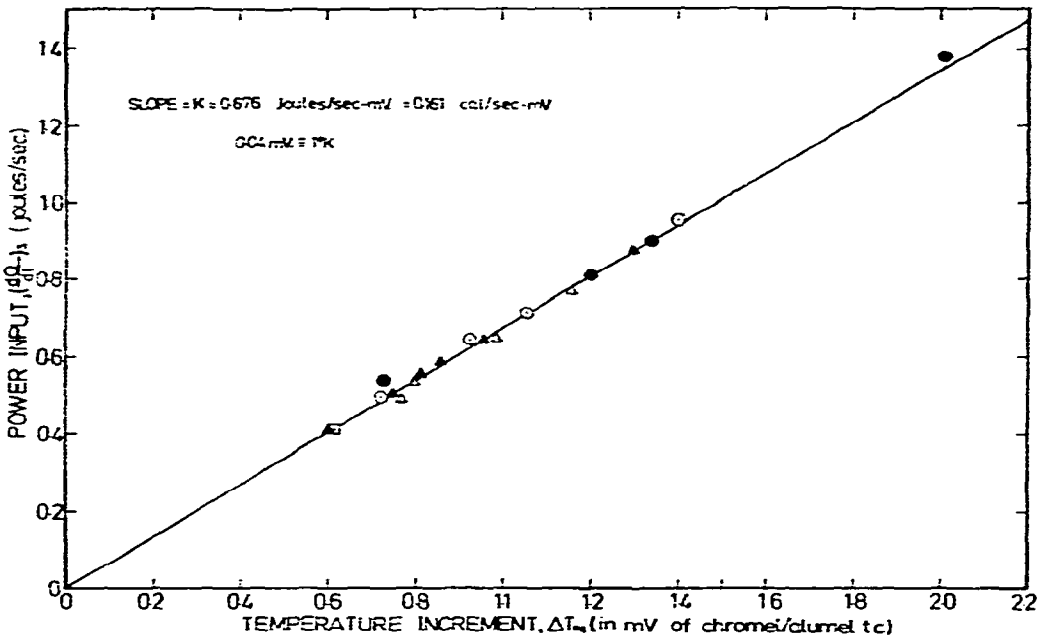

Fig. 3. Calibration data.

The treatment of data and typical detailed results may be illustrated by values obtained for the compound YSb. For an individual experiment the heat effect is obtained by the evaluation of eqn. (5) at any time after the completion of reaction; the heat transfer correction being obtained from the graphical evaluation of $\int_0^t \Delta T dt$ from a plot of ΔT vs. t such as shown in the lower part of Fig. 2. Since, if reaction has ceased and K correctly evaluated, the post-reaction decay of ΔT should be exactly compensated by the integrated heat transfer, eqn. (5) is normally evaluated at several intervals in the post-reaction period to confirm internal consistency. A typical series of calculations for a single run on YSb are shown in Table 1 and these demonstrate clearly the satisfactory constancy of the heat values so obtained. The results of a series of investigations of this compound are summarized in Table 2, together with those for LuSb and ScSb; the indicated uncertainty represents the calculated standard deviation ($|d_s|$) plus a 1% estimated calibration error. Also included in these tables are the temperature (T_r) at which reactions were observed to be initiated, together with the corresponding rates of heating $(dT/dt)_r$ at the time of reaction initiation.

TABLE 1

SPECIMEN EVALUATION

Sample: YSb

$M = 1486 \times 10^{-6}$ mol

$K/W = 0.0647$ min^{-1}

$T_f = 858$K; $T_{eq} = 831$K; $T_c = 760$K

t (min)	$\int_0^t \Delta T dt$ (mV min)	$\frac{K}{W}\int_0^t \Delta T dt$ (mV)	ΔT (mV)	$-\frac{Q}{W}$ (mV)
20	9.624	0.623	0.502	1.125
21	10.111	0.654	0.471	1.125
22	10.569	0.684	0.442	1.126
23	10.997	0.712	0.414	1.125
24	11.396	0.737	0.388	1.125
25	11.766	0.761	0.064	1.125
26	12.111	0.784	0.341	1.125
27	12.436	0.805	0.319	1.124
28	12.744	0.825	0.300	1.125
29	13.034	0.843	0.281	1.124
30	13.307	0.861	0.261	1.125
			Average	1.125

$W = 73$ cal mV^{-1} $= 307$ J mV^{-1}

$Q = -82.1$ cal $= 346$ J

$\Delta H = -55.3$ kcal mol^{-1} $= -233$ kJ mol^{-1}

In general, X-ray examination showed the reactions to have gone to completion and the product to have the NaCl structure; there were no indications of any side-reaction with the tantalum crucible. Satisfactorily reproducible results did prove more difficult to achieve in the experiments on ScSb. Evidence of incompleteness of reaction was encountered in a number of runs, necessitating the rejection of data from these. The results obtained in three satisfactory experiments with this compound are included in Table 2.

DISCUSSION

Comparatively few other measurements have been made of heats of formation of the family of NaCl phases occurring in the IIIA–VB alloy systems. However, in Table 3 the present data may be compared with those for the corresponding arsenides, studied by Faktor and Hanks[6], and with earlier data[5] for the nitrides of scandium, yttrium and lanthanum. An experimental value for LaSb is also included; this was obtained in vapour pressure studies in the authors' laboratory[9].

TABLE 2

HEATS OF FORMATION OF ScSb, YSb AND LuSb
1 cal = 4.184 J.

T_f (K)	T_{eq} (K)	T_r (K)	$\left(\frac{dT}{dt}\right)_r$ (deg min^{-1})	M (mol)	ΔH (kcal mol^{-1})	$\lvert d_3 \rvert$ (kcal mol^{-1})
Scandium antimonide						
889	861	764	9	0.002206	−31.7	0.3
896	873	734	15	0.001984	−33.3	1.9
889	861	762	11	0.002045	−29.1	2.3
				$\Delta H_{753} = -31.4 \pm 2.0$ kcal mol^{-1}		
Yttrium antimonide						
881	853	783	10	0.001818	52.4	0.6
857	840	784	8	0.001441	54.5	1.5
852	827	761	7.5	0.002158	51.6	1.4
858	831	760	9	0.001486	55.3	2.3
845	820	748	9	0.001106	51.3	1.7
				$\Delta H_{767} = -53.0 \pm 2.1$ kcal mol^{-1}		
Lutetium antimonide						
945	918	834	15	0.001613	45.5	0.8
888	861	735	17	0.002056	40.6	4.1
882	847	685	11	0.001567	47.9	3.2
				$\Delta H_{721} = -44.7 \pm 3.5$ kcal mol^{-1}		

While the formation of the antimonides is again strongly exothermic, it will be noted that their heats of formation are consistently smaller than those of the corresponding nitrides and arsenides. A more revealing comparison of the phases is to be expected, however, from an examination of their heats of atomisation, since reference to the monatomic vapours of the component elements provides a more uniform set of standard states. These quantities have, therefore, been calculated from the observed heats of formation using Hultgren's assessments of the heats of vapourisation of the elements[3]. The resulting values are given in Table 3 and it is interesting to consider these in relation to factors influencing the choice of phase structure. The relative stabilities of fourfold and sixfold co-ordinated structures in systems of this type have been discussed by Mooser and Pearson[1], using Pauling electronegativity differences (Δx) and the average principal quantum numbers ($\bar{n}$) as the phenomenological parameters, and by Phillips[2] in terms of the degree of ionicity of the bonding (f_i); the latter is defined by $f_i = C_{AB}^2/(E_h^2 + C_{AB})^2$, where E_h and C_{AB} are, respectively, the spectroscopically defined covalent and ionic energy gaps of the phase. Values of E_h and C_{AB} are normally obtained from experimental values of the dielectric constants[10], but, since such experimental data are not available for the present compounds, the

TABLE 3

LATTICE PARAMETERS, IONICITY PARAMETERS AND HEATS OF ATOMISATION AND FORMATION OF IIIA–VB NaCl STRUCTURES

1 cal = 4.184 J; 1 atomic unit = 5.29167×10^{-11} m; 1 eV = 1.6×10^{-19} J.

Compound	*ΔH formation* (*kcal mol*$^{-1}$)	*ΔH atomisation* (*kcal mol*$^{-1}$)	*Lattice parameter* (*atomic units*)	C_{AB} (*eV*)	E_h (*eV*)	f_i
ScN	71.2	274.5	8.409	8.7	5.5	.71
YN	71.5	286.0	9.218	7.8	4.4	.76
LaN	72.0	288.0	10.004	6.4	3.6	.76
LuN	72.2[a]	287.4[a]	9.006	8.2	4.6	.76
ScP	54.8[a]	224.9[a]	10.036	3.5	3.5	.49
YP	73.7[a]	255.0[a]	10.699	3.8	3.0	.62
LaP	72.2[a]	255.0[a]	11.385	3.3	2.6	.62
LuP	73[a]	255.0[a]	10.450	4.1	3.2	.62
ScAs	65.2	227.8	10.369	3.0	3.3	.45
YAs	77.4	251.2	10.993	3.4	2.9	.58
LaAs	73.0	248.3	11.597	3.0	2.5	.59
LuAs	75.2	249.7	10.733	3.6	3.0	.59
ScSb	31.4	185.0	11.071	1.9	2.8	.32
YSb	53.0	217.7	11.650	2.3	2.5	.46
LaSb	52.0	218.2	12.260	2.1	2.2	.48
LuSb	44.7	210.1	11.443	2.5	2.6	.48
ScBi	35.9[a]	176.3[a]	11.251	1.7	2.7	.28
YBi	66.3[a]	217.9[a]	11.778	2.2	2.4	.46
LaBi	62.5[a]	215.6[a]	12.430	1.9	2.1	.45
LuBi	65.6[a]	217.9[a]	11.640	2.3	2.5	.46

[a] Computed values.

parameters, E_h and C_{AB}, have been derived using analytical relationships established by Phillips'[2] and by Van Vechten's[10] studies of adamantine and rock-salt structures. Thus the average heteropolar energy gap, C_{AB}, may be computed from the formula

$$C_{AB} = b[(Z_A/r_A) - (Z_B/r_B)]\,e^{-K_s(r_A + r_B)/2}$$

where Z_A and Z_B are the valencies and r_A and r_B the effective covalent radii of A and B, respectively; K_s is the Thomas–Fermi screening wave number and is defined by $K_s = 4K_f/\pi a_0$, where K_f is the Fermi momentum of a free electron gas of density equal to that of the valence electrons and a_0 is the Bohr radius. The covalent radii are themselves defined by relations of the form

$$r_A = r_{IV}(a_{AB}/a'_{AB})$$

where r_{IV} is the single bond covalent radius of the Group IV element belonging to the same row of the Periodic Table, a_{AB} is the observed lattice constant of the compound and a'_{AB} the lattice constant which would be predicted from the covalent radii of the corresponding Group IV elements. b is a dimensionless parameter which is empiri-

cally related to the deviation of the actual lattice constant (a_{AB}) from the predicted "normal covalent value" (a'_{AB})[10]. Values of the homopolar energy gap (E_h) may be estimated on the basis of the assumption that this is a function of the nearest neighbour distance only. Examination of the data for NaCl structures, presented by Van Vechten[10], suggest the existence of the empirical relation

$$E_h = 1056 a_{AB}^{-2.48} + 0.08$$

where a_{AB} is the lattice constant of the compound, expressed in atomic units.

Lattice parameters are available for all the IIIA–VB NaCl structures[11] and these are assembled in Table 3. They have been used, together with the equations outlined above, to obtain the values of C_{AB} and E_h for these compounds and these are also shown in this table. Finally, the ionicity values, f_i, indicating the fraction of ionic character expected in the bonding have been calculated and are also tabulated.

Surprisingly, in view of their sizable exothermic heats of formation, stable NaCl structures are not, at first sight, favoured in most of the present systems by either the Mooser and Pearson or Phillips criteria. The average principal quantum numbers and the Pauling electronegativity differences suggest that conditions are favourable only for the nitrides, for the lanthanum compounds and for YBi and LuBi; LuSb, LuAs and LuP are in a borderline state, while the remaining scandium and yttrium compounds have unfavourable values of the Mooser and Pearson parameters. Similarly, the fractional ionicity values, given in Table 3, imply that only the nitrides approach the Phillips' criterion, ($f_i(AB) \geqslant 0.785$), for the NaCl structure, while, of the remainder, the compounds involving scandium or antimony appear likely to be the least stable. The persistence of the NaCl structures into the regions where the above criteria would otherwise suggest more directionally bonded structures is probably attributable to the lack of p character in the bonding orbitals of the IIIA elements; this would inhibit the formation of hybrids suitable for tetrahedral bonding. Similar effects have been noted[1] with the later transitional metals, where NiAs structures occur in the adamantine regions of the Mooser–Pearson plot, again because their bonding hybrids favour octahedral rather than tetrahedral co-ordination. That the NaCl structure, rather than the NiAs type, is adopted under similar circumstances in the present systems is undoubtedly due to the involvement of larger electronegativity differences and, hence, greater polarities; by adopting the NaCl structure a better separation of like ions is achieved.

Despite this deviation from the simplest criteria, it is noted that the observed heats of atomisation are generally consistent with the relative stabilities of the phases suggested by their positions in ($\bar{n}$ vs. Δx) or (C_{AB} vs. E_h) plots. Thus, since Phillips and Van Vechten[12] have been able to predict heats of formation of tetrahedrally co-ordinated compounds using spectroscopically defined ionicities, an inter-relation of phase stability and bond character may be expected for the NaCl phases. The nature of this is examined in Fig. 4 where the heats of atomisation, of the eleven examples for which experimental data are available, are plotted versus their corresponding f_i values. An essentially linear inter-dependence is indicated and this may be satis-

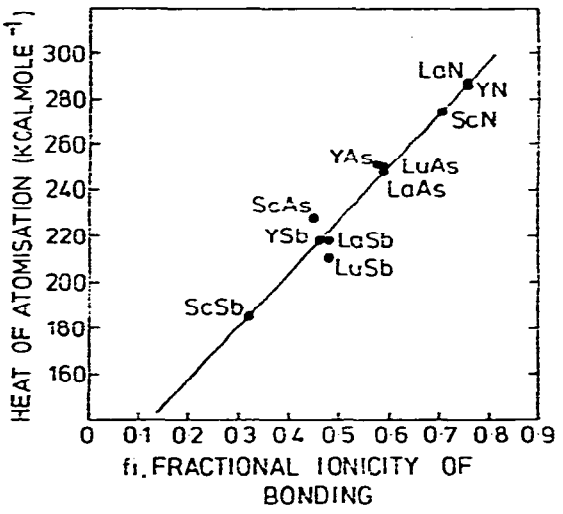

Fig. 4. Inter-relation of heats of atomisation and ionicity of bonding: IIIA–VB NaCl structures.

factorily represented by the relation, ΔH (atomisation) (kcal/mole) $= 111.5 + 231.4 \times f_i$, derived by least square analysis of the data. This relationship appears to be obeyed over a sufficiently large range of ionicity values to justify its use to estimate heat data for the remaining uninvestigated IIIA–VB NaCl phases. Heats of atomisation of the phosphides, of the bismuthides and of LuN have been so obtained using their f_i values already computed. Finally the heats of formation of these phases have been calculated by combining these with the heats of vapourisation of the elements. The estimated heat data are again to be found in Table 3.

ACKNOWLEDGEMENT

The research programme of which this work forms part was supported by the United Kingdom Ministry of Technology under Agreement No. 2027/048/RL.

REFERENCES

1 E. Mooser and W. B. Pearson, *Acta Crystallogr.*, 12 (1959) 1015.
2 J. C. Phillips, *Rev. Mod. Phys.*, 42 (1970) 317.
3 R. Hultgren, R. L. Orr, F. D. Anderson and K. K. Kelley, *Selected Values of the Thermodynamic Properties of Metals and Alloys*, Wiley, New York, 1963.
4 N. Sclar, *J. Appl. Phys.*, 33 (1962) 2999.
5 O. Kubaschewski, E. Ll. Evans and C. B. Alcock, *Metallurgical Thermochemistry*, 4th ed., Pergamon, London, 1967.
6 R. Hanks and M. M. Faktor, *Trans. Faraday Soc.*, 63 (1967) 1130.
7 J. N. Pratt and K. S. Chua, "Thermodynamic Studies of Some Rare-Earth Alloys", Final Report, Min. Tech. Agreement No. 2027/048, University of Birmingham, 1970.
8 O. Kubaschewski and R. Hultgren, in H. A. Skinner (editor), *Experimental Thermochemistry*, Interscience, New York, 1962, p. 343.
9 J. N. Pratt and D. T. Underhill, unpublished work, University of Birmingham, 1972.
10 J. A. Van Vechten, *Phys. Rev.*, 182 (1969) 891.
11 *Landolt-Börnstein Tables*, (New Series), Group III, Vol. 6, *Structure Data*, Springer-Verlag, Heidelberg, 1971.
12 J. C. Phillips and J. A. Van Vechten, *Phys. Rev. B*, 2 (1970) 2147.